# Note on Earhtquake Seismology <2> Crack theory and fracture

Hideo Aochi

1. Quantitaive Framework
2. Crack theory and fracture
3. Friction
4. Numerical model
5. Earthquake scaling
6. Obsevational seismology

8 December 2025

# Crack theory

2D-SH (Model III) problem

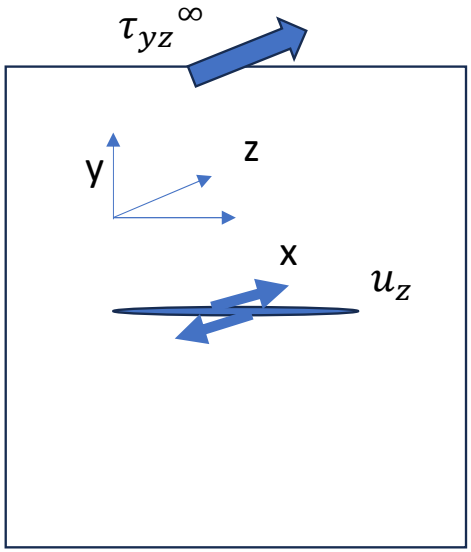


$$\frac{\partial \tau_{xz}}{\partial x} + \frac{\partial \tau_{yz}}{\partial y} = 0$$

$$\varepsilon_{xz} = \frac{\partial u_z}{\partial x}, \varepsilon_{yz} = \frac{\partial u_z}{\partial y}$$

$$\tau_{xz} = \mu \varepsilon_{xz}, \tau_{yz} = \mu \varepsilon_{yz}$$

$$\nabla^2 u_z = \frac{\partial^2 u_z}{\partial x^2} + \frac{\partial^2 u_z}{\partial y^2} = 0$$

$$\tau_{yz} = -\Delta\tau \equiv \tau_{yz}(x) - \tau_{yz}{}^{\infty}; -c \leq x \leq c; y = 0$$

Analytically solved.

$$\tau_{yz} = -\frac{1}{\pi\sqrt{x^2 - c^2}} \int_{-c}^{+c} \frac{\Delta\tau(x')\sqrt{c^2 - x'^2}}{x - x'} dx'$$

Expansion around crack tip: $\zeta - c \equiv re^{i\theta}$

$$\tau_{yz} \cong \frac{K_{III}}{\sqrt{2\pi r}} \cos\left(\frac{\theta}{2}\right); \; u_z \cong \frac{2K_{III}}{\mu} \sqrt{\frac{r}{2\pi}} sin\left(\frac{\theta}{2}\right)$$

$$K_{III} = \frac{1}{\sqrt{\pi c}} \int_{-c}^{+c} \Delta\tau(x') \sqrt{\frac{c + x'}{c - x'}} dx'$$

$K_{III} = \tau_{yz}^{\infty}\sqrt{\pi c}$ if $\Delta\tau(x') = \tau_{yz}^{\infty}$

# Dislocation theory

Burgers vector b $f_j = \frac{\mu b}{2\pi} \frac{1}{x_j - x_i}$ Force at j-th atom by i-th atom.

$$\frac{\mu b}{2\pi} \int_{-c}^{+c} \frac{f(x')}{x - x'} dx' + \tau^{\infty} = \tau(x); -c \leq x \leq c$$

f(x) : dislocation density function

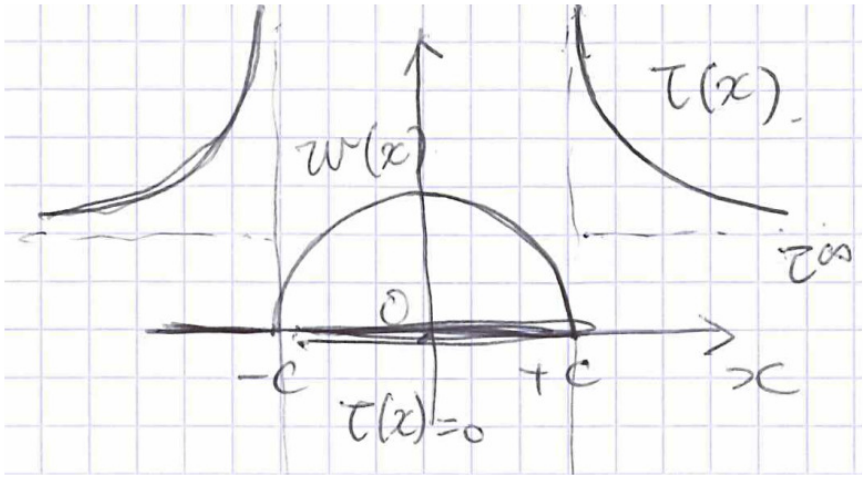


$$w(x) = \frac{2\tau^{\infty}}{\mu} \sqrt{c^2 - x^2}; -c \leq x \leq +c$$

$$\tau(x) = 0; -c \leq x \leq +c$$

$$\tau(x) = \tau^{\infty} + \tau^{\infty} \left( \frac{x}{\sqrt{x^2 - c^2}} - 1 \right); \ |x| > c$$

# Griffith's criterion (1920)

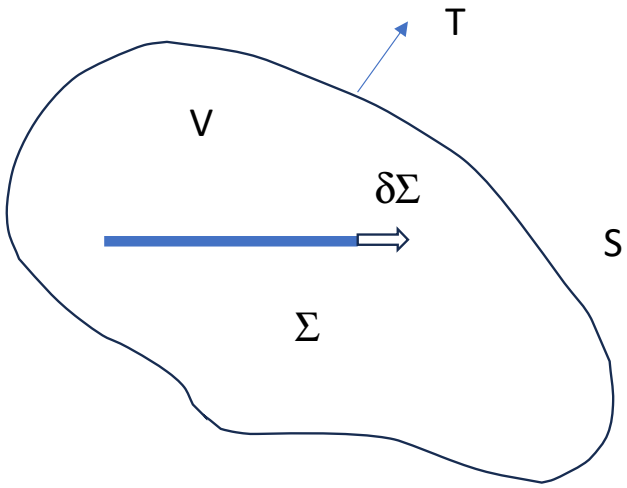


$$\delta E + \delta K = \delta W + \delta Q - \delta \Pi$$

Elastic strain energy + kinetic energy

Work done by T + heat flux by S + Energy needed to create δΣ

$$-\delta(E - W) = \delta \Pi$$

Potential energy of system = Energy needed to create δΣ

Energy release rate: $G \equiv -\frac{d(E-W)}{d\Sigma}$

Fracture surface energy $G_c \equiv \frac{d\Pi}{d\Sigma}$

$G > G_c$ ⟹ Spontenous rupture growth

$$G_{III} = \frac{1}{2\mu} {K_{III}}^2$$

# From static to moving crack.

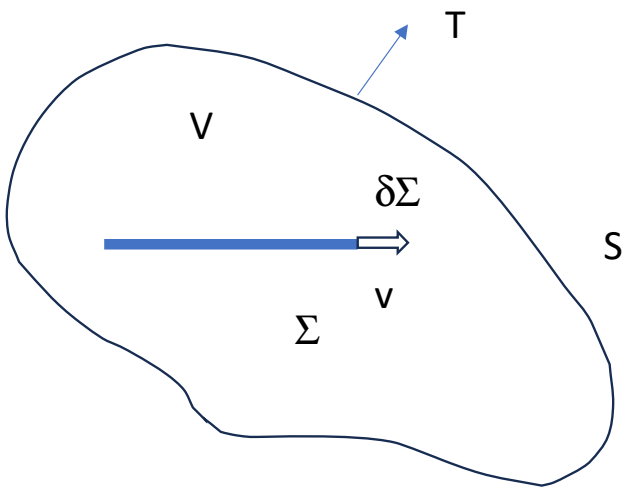


Dynamic stress intensity factor: $K_d(v) = f(v)K_s$

$$K_{III\,d} = \sqrt{1-\left(\frac{v}{\beta}\right)^2}\,K_s, \qquad K_{II\,d} \sim (1 - v/\beta)K_s$$

For mode III

$$G_d(v) = \frac{1}{2\mu}\frac{\sqrt{1-v/\beta}}{\sqrt{1+v/\beta}}{K_s}^2$$

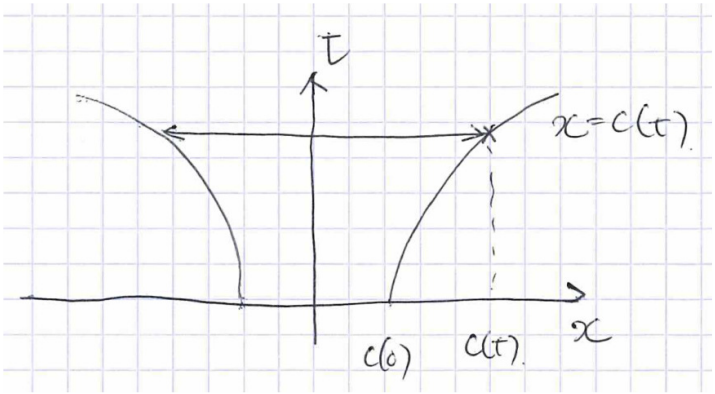


$$K_s = \sqrt{\frac{2}{\pi}}\int_{c-\beta t}^{c}\frac{\Delta\tau(x', t-\frac{c-x'}{\beta})}{\sqrt{c-x'}}\,dx'$$

v=dc/dt

# J-integral

Potential energy $$U \equiv E - W = \int_S \varepsilon dS - \int_\Gamma \vec{T} \cdot \vec{u}\, d\Gamma$$

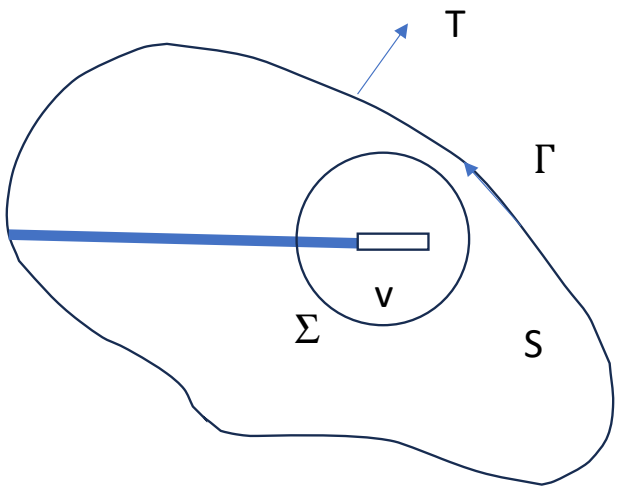


Breakdown zone

$$G = -\lim_{\delta x \to 0} \frac{1}{\delta x} \int_S \{\varepsilon(\varepsilon_{ij}) - \varepsilon(\varepsilon_{ij} + \delta\varepsilon_{ij}) + (\sigma_{ij} + \delta\sigma_{ij})\delta\varepsilon_{ij}\} dS$$

$$G = \int_\Gamma \left[ n_x \varepsilon - \vec{T} \cdot \frac{\partial \vec{u}}{\partial x} \right] d\Gamma \equiv J + \text{invariant}$$

Rice (1968)

$$G = \frac{1}{2\mu} K^2$$

On the dislocation. $$J(\Gamma_c) = -\int_\Sigma \tau \frac{\partial w}{\partial x} dx = \int_0^{D_c} \tau(w) dw = G_c; if\ any\ \tau = \tau(w)$$

# Cohesive Force across the Tip of a Longitudinal-Shear Crack and Griffith's Specific Surface Energy

YOSHIAKI IDA

*Department of Earth and Planetary Sciences*
*Massachusetts Institute of Technology, Cambridge, Massachusetts 02139*

The cohesive force across the fault plane is considered in order to understand the physical mechanism of rupture at the tip of a longitudinal-shear crack. The elastic field around the tip of a crack and the condition of rupture growth are systematically derived from the assumption that the cohesive force is given as a function of the displacement discontinuity. This assumption is more physically meaningful than those originally used by G. I. Barenblatt in 1959 and 1962. The stress field around the tip is calculated for several models of cohesive force, and is shown to be nonsingular even at the tip. The condition of rupture growth that is used to determine the rupture velocity turns out to be equivalent to the Griffith criterion and the relation employed by B. V. Kostrov in 1966, but the specific surface energy is defined more clearly in this paper.

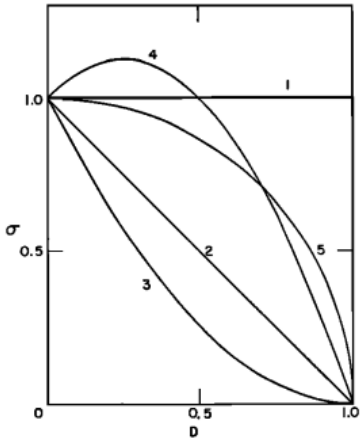


Fig. 1. The models of the cohesive force $\sigma(D)$ used for numerical calculations. The number attached with each curve corresponds to the model in Table 1.

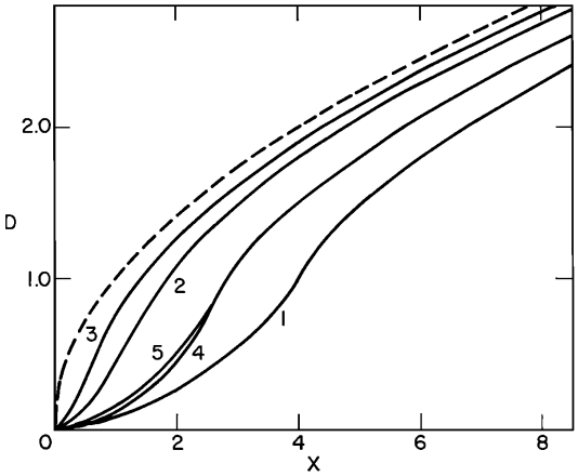


Fig. 2. The displacement discontinuity $D$ around the tip ($X = 0$) of a crack for the models given in Table 1. The dashed curve gives the solution for the case of no cohesive force.

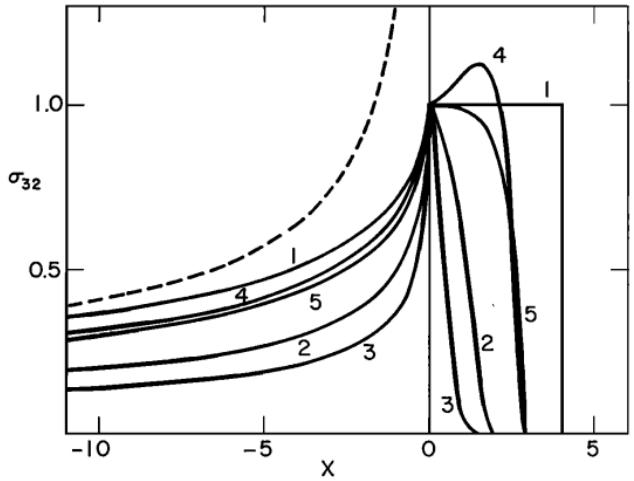


Fig. 4. The stress component $\sigma_{32}$ around the tip ($X = 0$) of a crack for the models given in Table 1. The dashed curve gives the solution for the case of no cohesive force.

# Cohesive force

Orowan (1948), Gilman, (1959)

Tension between two atoms $F = f_0 \cdot \sin\left(\frac{2\pi(a-a_0)}{\lambda}\right) \sim f_0\left(\frac{2\pi(a-a_0)}{\lambda}\right)$

Distance: a

Hooke's law: $F = E \cdot \left(\frac{(a-a_0)}{a_0}\right)$ ➡ $f_0 = \frac{\lambda}{2\pi}\frac{E}{a_0}$

$$G_c = \int_0^{\lambda/2} f_0 \sin\left(\frac{2\pi(a-a_0)}{\lambda}\right) d\delta = \frac{\lambda f_0}{\pi} \quad \Rightarrow \quad f_0 = \sqrt{\frac{EG_c}{2a_0}}$$

$f_0 \sim E/10$ (theoretical upper limit)

Computers and Geotechnics 183 (2025) 107239

Contents lists available at ScienceDirect

Computers and Geotechnics

journal homepage: www.elsevier.com/locate/compgeo

Research Paper

# Nanoscale contact behavior of $\alpha$-quartz asperities — A molecular dynamics approach

Sheng Li [a,*], Eiichi Fukuyama [a,b]

[a] Department of Civil and Earth Resources Engineering, Kyoto University, Kyoto, Japan
[b] National Research Institute for Earth Science and Disaster Resilience, Tsukuba, Japan

ARTICLE INFO

*Keywords:*
Nanoscale
$\alpha$-Quartz asperities
Contact deformation
Contact models
Molecular dynamics

ABSTRACT

Rock surfaces are composed of asperities at various scales. Accurate modeling of the multiscale contact deformation of asperities is of great importance to study the earthquake source mechanics and hydraulic properties of fractures. In this study, to shed light on the nanoscale contact behavior of rock asperities that might not have been paid much attention to in previous studies, we simulated a series of nanoscale contact processes of $\alpha$-quartz asperities under single-asperity contact employing molecular dynamics method. In addition to the investigation of the influence of contact configuration and asperity size on the asperity failure, we compared the simulation results with macroscopically elastic and elastoplastic contact models to evaluate the multiscale applicability. We observed that fracture occurs in the nanoscale $\alpha$-quartz asperities during contact process, inconsistent with the traditional assumptions of elastic and elastoplastic deformation of rock asperities. Moreover, the asperity size and contact configuration significantly affect the failure mechanism of $\alpha$-quartz asperities, specifically the transition from plasticity-dominant failure to fracture damage. Finally, a multiscale disparity exists, where macroscopic contact models are limited to predict the nanoscale contact behavior of $\alpha$-quartz asperities. The results obtained here underscore the need to re-evaluate the assumptions of rock asperity deformation and emphasize the importance of considering contact configurations and multiscale effects of rock asperities.

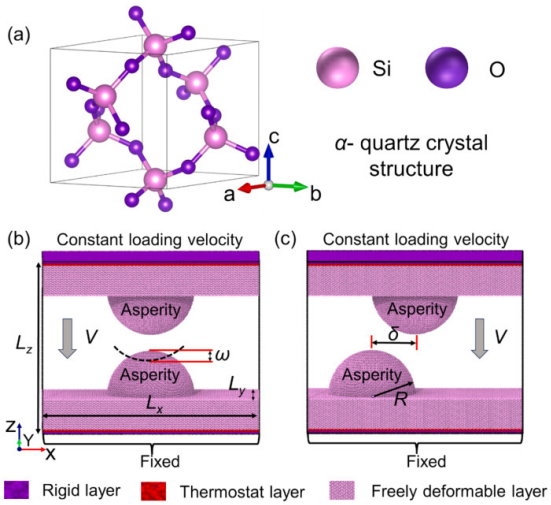


**Fig. 1.** A schematic illustration of crystal structure of α-quartz and the contact configuration of asperities. (a) The crystal structure of α-quartz (visualized by VESTA, Momma & Izumi, 2011). (b) The model with asperity top center symmetry. $\omega$ is the interference distance after contact. $L_x$, $L_y$ and $L_z$ stand for the dimension of model space. $V$ is the loading velocity in the normal direction. (c) The model with asperity top center offset. $\delta$ is the offset distance between asperity tops. $R$ is the asperity radius.

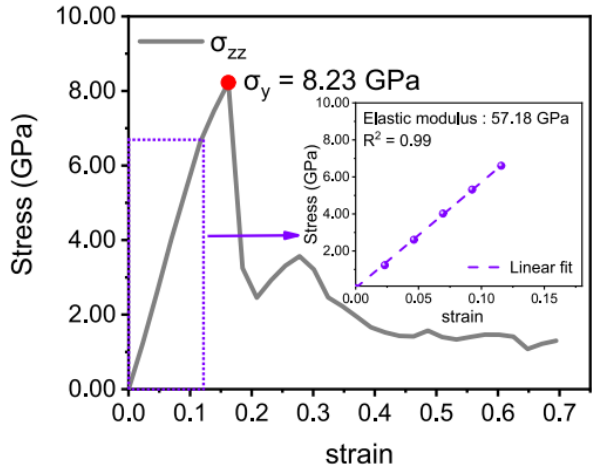


**Fig. 2.** Stress–strain curve from uniaxial compression test in MD simulation. Red point corresponds to the yield strength. The detailed data in the purple dotted square are shown in an inset plot. (For interpretation of the references to colour in this figure legend, the reader is referred to the web version of this article.)

# Mohr-Coulomb diagram

Byerlee's law (1967)

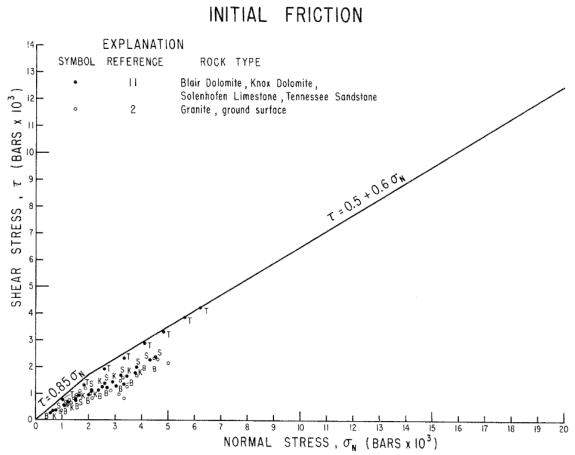


Shear stress

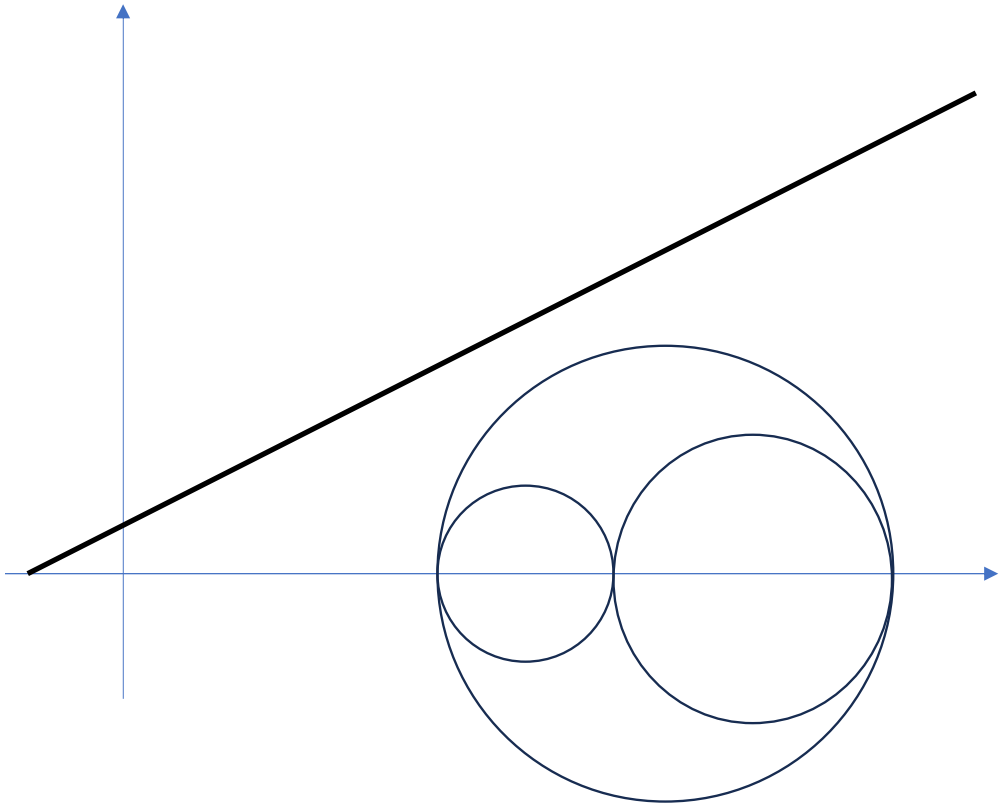

Normal stress

# Mohr-Coulomb diagram

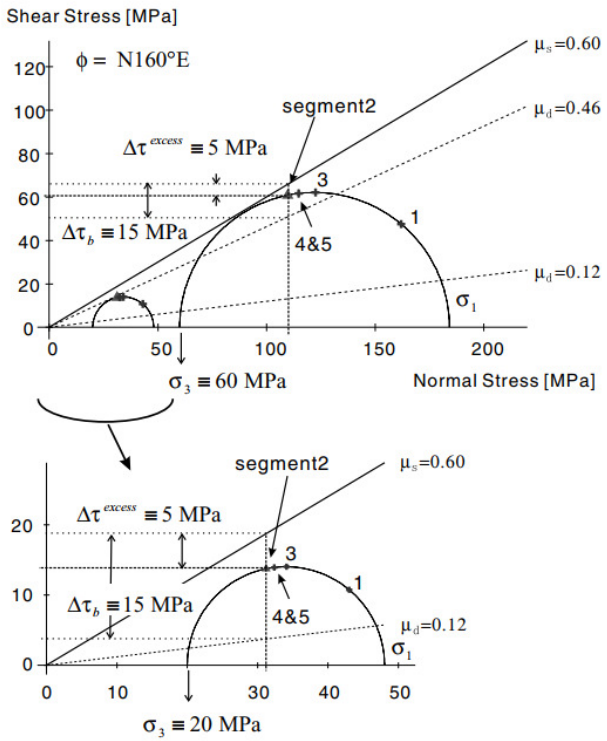


**Figure 3.** Initial stress situations for the cases $|\sigma_3| = 60$ MPa and 20 MPa, respectively, supposing $\Phi = $ N 160°E, $R = 0$, $\Delta\tau_b = 15$ MPa and $\tau^{excess} = 5$ MPa. Triangles represent Segment 2 as the reference segment in this tectonic stress regime and other marks show the other segments. Their relative positions on the Mohr circle do not change with the value of $|\sigma_3|$, but do change with respect to the dynamic friction line of $\mu_d$. See the text for details and Appendix A for all the other values of $\Phi$.

Aochi et al. (2006)

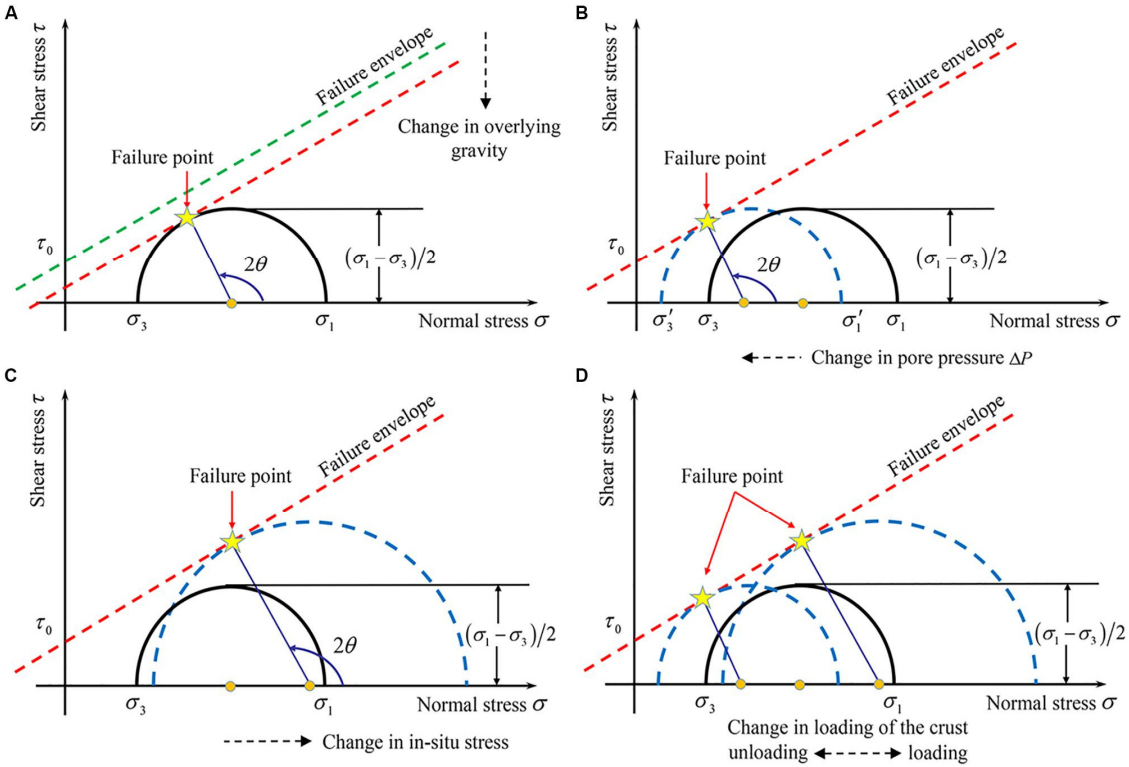


Doglioni (2018), He et al. (2020)

# Further reading


- Freud (1989). Dynamic fracture mechanics. Cambridge University Press.